Case Report

A case of focal nodular hyperplasia-like lesion presenting unusual signal intensity on the hepatobiliary phase of gadoxetic acid-enhanced magnetic resonance image ☆

Kumi Ozaki, MD, PhD[a,h,*], Norihide Yoneda, MD, PhD[b], Kenichi Harada, MD, PhD[c], Hiroshi Ikeno, MD, PhD[b], Misa Takahashi, MD[d], Yasuharu Kaizaki, MD, PhD[e], Kazuya Maeda, MD[f], Shohei Higuchi, MD[e,g], Kenji Takata, MD, PhD[a], Toshifumi Gabata, MD, PhD[b]

[a] Departments of Radiology, Faculty of Medical Sciences, University of Fukui, Fukui, Japan
[b] Department of Radiology, Kanazawa University Graduate School of Medicine, Kanazawa, Japan
[c] Department of Pathology, Kanazawa University Graduate School of Medicine, Kanazawa, Japan
[d] Department of Radiology, Toyama City Hospital, Toyama, Japan
[e] Departments of Pathology, Fukui Prefectural Hospital, Fukui, Japan
[f] Departments of Gasterointestinal Surgery, Fukui Prefectural Hospital, Fukui, Japan
[g] Departments of Pathology, Faculty of Medical Sciences, University of Fukui, Fukui, Japan
[h] Department of Radiology, Hamamatsu University School of Medicine, Hamamatsu, Japan

ARTICLE INFO

ABSTRACT

Focal nodular hyperplasia (FNH) or FNH-like lesions of the liver are benign lesions that can be mostly diagnosed by hepatobiliary phase gadoxetic acid-enhanced magnetic resonance imaging (MRI). Accurate imaging diagnosis is based on the fact that most FNHs or FNH-like lesions show characteristic hyper- or isointensity on hepatobiliary phase images. We report a case of an FNH-like lesion in a 73-year-old woman that mimicked a malignant tumor. Dynamic contrast-enhanced computed tomography (CT) and MRI using gadoxetic-acid revealed an ill-defined nodule showing early enhancement in the arterial phase and gradual and prolonged enhancement in the portal and equilibrium/transitional phases. Hepatobiliary phase imaging revealed inhomogeneous hypointensity, accompanied by a slightly isointense area compared to the background liver. Angiography-assisted CT showed a portal perfusion defect of the nodule, inhomogeneous arterial blood supply in the early phase, and less internal enhancement in the late phase, accompanied by irregularly shaped peritumoral enhancement. No central stellate scar was identified in any of the images. Imaging findings could not exclude the possibility of hepatocellular carcinoma, but the nodule was

---

pathologically diagnosed as an FNH-like lesion by partial hepatectomy. In the present case, an unusual inhomogeneous hypointensity on hepatobiliary phase imaging made it difficult to diagnose the FNH-like lesions.

Introduction

Focal nodular hyperplasia (FNH) is the liver's second most common benign lesion. When FNH manifests without all the typical pathological features or occurs in the context of abnormal liver, nodules are referred to using expressions such as "FNH-like [1–3]." Both have similar histological structures and do not require specific treatments. An accurate imaging diagnosis of FNH and FNH-like lesions can prevent unnecessary interventions, such as biopsy or surgery, and waste of medical resources.

The approval of gadoxetic acid, a liver-specific MR contrast agent, has dramatically improved the accuracy of diagnosis of focal liver lesions, including FNH and FNH-like lesions [4]. Gadoxetic acid is a dual-function contrast agent that combines the properties of an extracellular contrast agent for dynamic imaging with a hepatocyte-specific agent. Approximately 50% of the injected dose is taken up by functioning hepatocytes and excreted in the bile, thus enabling tumor characterization

Table 1 – Laboratory data.					
WBC	5200	/μL	Amy	89	IU/L
RBC	388×10^4	/μL	TG	149	mg/dL
Hb	9.2	g/dL	K	4.1	mEg/L
Ht	41.6	%	Na	140	mEg/L
Plt	25.1×10^4	/μL	Cl	107	mEg/L
			Ca	9.1	mEg/L
BUN	13	mg/dL	P	3.5	mEg/L
Cr	0.56	mg/dL			
CRP	0.13	mg/dL	CEA	1.9	ng/mL
T-bil	0.5	mg/dL	CA19-9	21.3	U/mL
AST	27	U/L	AFP	2.2	ng/mL
ALT	32	U/L	AFP-L3	< 0.5	%
LDH	191	U/L	PIVKA-2	13	mAU/mL
ALP	218	U/L			
γGTP	43	U/L	HBsAg	–	
TP	7.0	g/dL	HBsAb	–	
Alb	4.3	g/dL	HBcAb	–	
T-cho	156	mg/dL	HCVAb	–	

WBC, white blood cells; RBC, red blood cells; Hb, hemoglobin; Ht, hematocrit; Plt, platelets; BUN, blood urea nitrogen; Cr, Creatinine; CRP, C-reactive protein; T-bil, total bilirubin; AST, aspartate transaminase; ALT, alanine transaminase; LDH, lactate dehydrogenase; ALP, alkaline phosphatase; γGTP, gamma-glutamyl transpeptidase; TP, total protein; Alb, albumin; T-cho, T-cholesterol; Amy, Amylase; CEA, carcinoembryonic antigen; CA19-9, carbohydrate antigen 19-9; AFP, alpha fetoprotein; PIVKA-2, protein induced by vitamin K absence/antagonist-II; HBsAg, hepatitis B surface antigen; HBsAb, hepatitis B surface antibody; HBcAb, hepatitis B core antibody; HCVAb, hepatitis C virus antibody.

Fig. 1 – Dynamic contrast-enhanced computed tomography (CT). (A) On noncontrast-enhanced CT, an ill-defined nodule of 15 mm in largest diameter was identified in segment 8 and showed hypodensity compared to background liver parenchyma (arrow). (B–D) On dynamic contrast-enhanced CT, the nodule shows early enhancement at the arterial phase and gradual and prolonged enhancement at the portal and equilibrium phases (arrows).

according to the presence or absence of functioning hepatocytes [5].

The pathogenesis of FNH or FNH-like lesion is a local reactive hyperplastic response of hepatocytes to abnormal hepatic blood flow [6,7]. Based on this pathogenesis, FNH and FNH-like lesions comprise benign hepatocytes that maintain hepatocyte function. Therefore, the vast majority (94%-97%) of FNH/FNH-like lesions show both uptake of gadoxetic acid and hyper- or iso-intensity on the hepatobiliary phase [4], and magnetic resonance imaging (MRI) using gadoxetic acid increased the accuracy of imaging diagnosis of FNHs. Conversely, when the hypervascular nodule does not show characteristic high or iso-intensity in the hepatobiliary phase, diagnosing FNH or FNH-like lesions is difficult.

Herein, we report a case of an FNH-like lesion that was difficult to diagnose due to unusual findings of gadoxetic acid on hepatobiliary phase images that could be correlated with pathological specimens including OATP1B3 expression.

Case report

A 73-year-old woman with acute pancreatitis underwent contrast-enhanced abdominal computed tomography (CT) to assess the severity index, and a hepatic mass was incidentally detected. The patient had a daily drinking habit (more than 60 g of alcohol per day) for over 20 years but had no history of chronic liver disease, including alcohol-related liver disease. A physical examination on admission yielded unremarkable findings 2 months after treating acute pancreatitis. Laboratory data, including inflammatory reactions, pancreatic enzymes, and hepatobiliary enzymes, were within normal ranges. Tests for hepatitis B and C viral antibodies were negative. Serum tumor markers and other markers were within normal ranges (Table 1).

The ultrasound image could not depict the nodule because it was just under the diaphragm. On noncontrast-enhanced CT, an ill-defined nodule with the largest diameter of 15 mm was identified in segment 8 and showed hypodensity compared with the background liver parenchyma (Fig. 1A). On dynamic contrast-enhanced CT, the nodule showed early enhancement in the arterial phase and gradual and prolonged enhancement in the portal and equilibrium phases (Figs. 1B–D). MRI was performed 2 months after the CT examination, and no changes in size were observed. The nodule appeared hypointense without focal fat deposition on T1-weighted imaging (in and out of phase) (Figs. 2A and B). The nod-

ule showed moderate hyperintensity compared to the background liver on fat-suppressed T2-weighted imaging (Fig. 2C) and slight hyperintensity on diffusion-weighted imaging (b value, 800) (Fig. 2D). Precontrast T1-weighted imaging with fat suppression showed hypointensity (Fig. 2E).

In a dynamic contrast-enhanced study using gadoxetic acid (Gd-EOB-DTPA; Primovist, Bayer Schering Pharma, Germany), early enhancement in the arterial phase and gradual and prolonged enhancement at the portal and transitional phases were observed on MRI (Figs. 2F–H). Hepatobiliary phase imaging revealed inhomogeneous hypointensity, accompanied by a slightly isointense area compared to the background liver (Fig. 2I).

Hemodynamic evaluation using angiography-assisted CT showed portal perfusion defects of the nodule and surrounding liver parenchyma on CT during arterial portography (Fig. 3A). On CT during hepatic arteriography, the nodule showed an inhomogeneous arterial blood supply in the early phase and less internal enhancement in the late phase than in the early phase (Figs. 3B and C). Surrounding the liver parenchyma of the nodule was accompanied by an irregular portal perfusion defect, less arterial blood supply than that of the nodule in the early phase, and a similar arterial blood supply in the late phase to that of the early phase (Figs. 3A–C). Five minutes after injection of the contrast material, prolonged enhancement of the nodule was not identified, and the enhancement of the surrounding liver parenchyma disappeared (Fig. 3D). Venous drainage directly connected to the
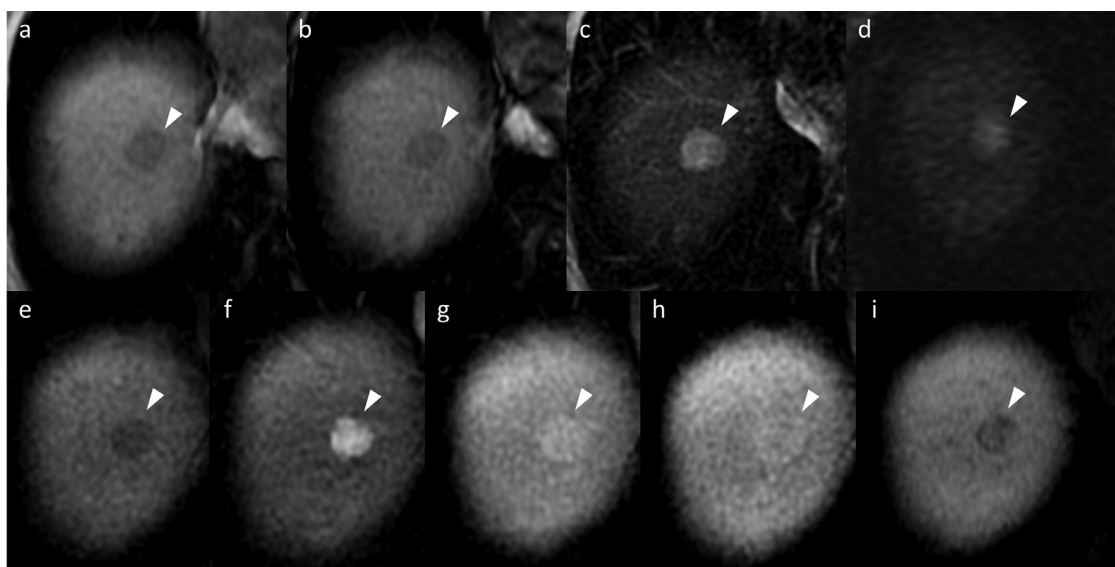

Fig. 2 – Dynamic contrast-enhanced magnetic resonance (MR) imaging using gadoxetic acid. (A, B) T1-weighted images (in and out of phase) (A, in phase; B, out of phase). The nodule shows hypointensity (arrowheads), and focal fat deposits within the mass are not identified. No central stellate scar was identified during any phase. (C) The nodule appears hyperintense compared to the background liver on fat-suppressed T2-weighted imaging (arrowhead). (D) The nodule appeared slightly hyperintense compared with the background liver on diffusion-weighted imaging (b value, 800) (arrowhead). (E) The nodule appears hypointense on the precontrast T1-weighted image with fat suppression (arrowhead). (F–H). On the dynamic contrast-enhanced study, early enhancement in the arterial phase (F), and gradual and prolonged enhancement in the portal (G) and transitional (H) phases (arrowheads), as seen on CT. (I) Hepatobiliary phase image reveals inhomogeneous hypointensity accompanying a slightly isointense area compared to the background liver (arrowhead). The dotted isointense areas are scattered within the nodule.
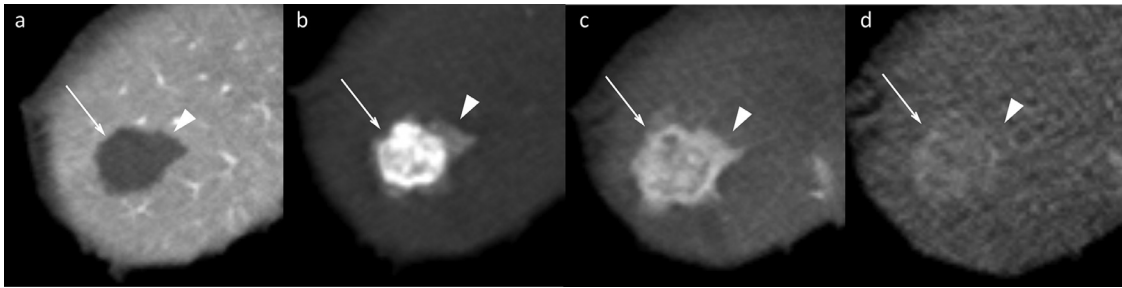
Fig. 3 – Angiography-assisted computed tomography (CT) (A) CT during arterial portography appears portal perfusion defect of the nodule and surrounding liver parenchyma. (B) On CT during hepatic arteriography, the nodule shows inhomogeneous arterial blood supply (arrow), accompanying irregular area (arrowhead) shows less arterial blood supply than the nodule at the early phase. (C) At the delayed phase of CT during hepatic arteriography, the nodule shows an inhomogeneous low arterial blood supply than that at the early phase (arrow). The irregularly shaped area surrounding the nodule shows more arterial blood supply than that of the early phase (arrowhead). (D) Five minutes after injection of contrast material, prolonged enhancement of the nodule was not identified (arrow), and the enhancement of the surrounding liver parenchyma disappeared (arrowhead). No central stellate scar was identified at any phase.
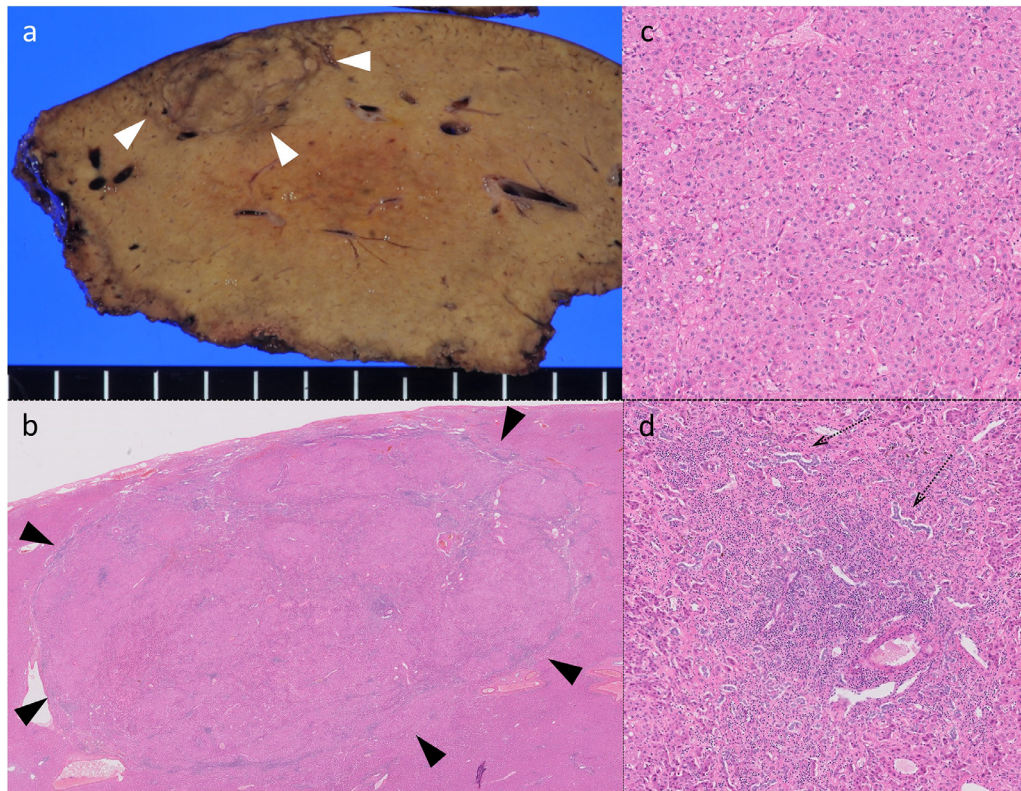
Fig. 4 – Macroscopic and microscopic findings of the resected specimen. (A) The resection specimen shows an ill-defined tonal nodule, similar to that of the surrounding liver parenchyma (arrowheads). (B) The nodule (arrowheads) shows a similar tone to that of the surrounding liver parenchyma. Neither fibrous capsule nor central fibrous scar was identified (hematoxylin and eosin [HE] staining, original magnification, x 10). (C) The nodule consists of cell proliferation without nuclear atypia, similar to normal hepatocytes (HE staining, original magnification, x 40). (D) Ductular proliferation (arrows) and unpaired arteries (not shown) were identified (HE staining; original magnification, x 40).
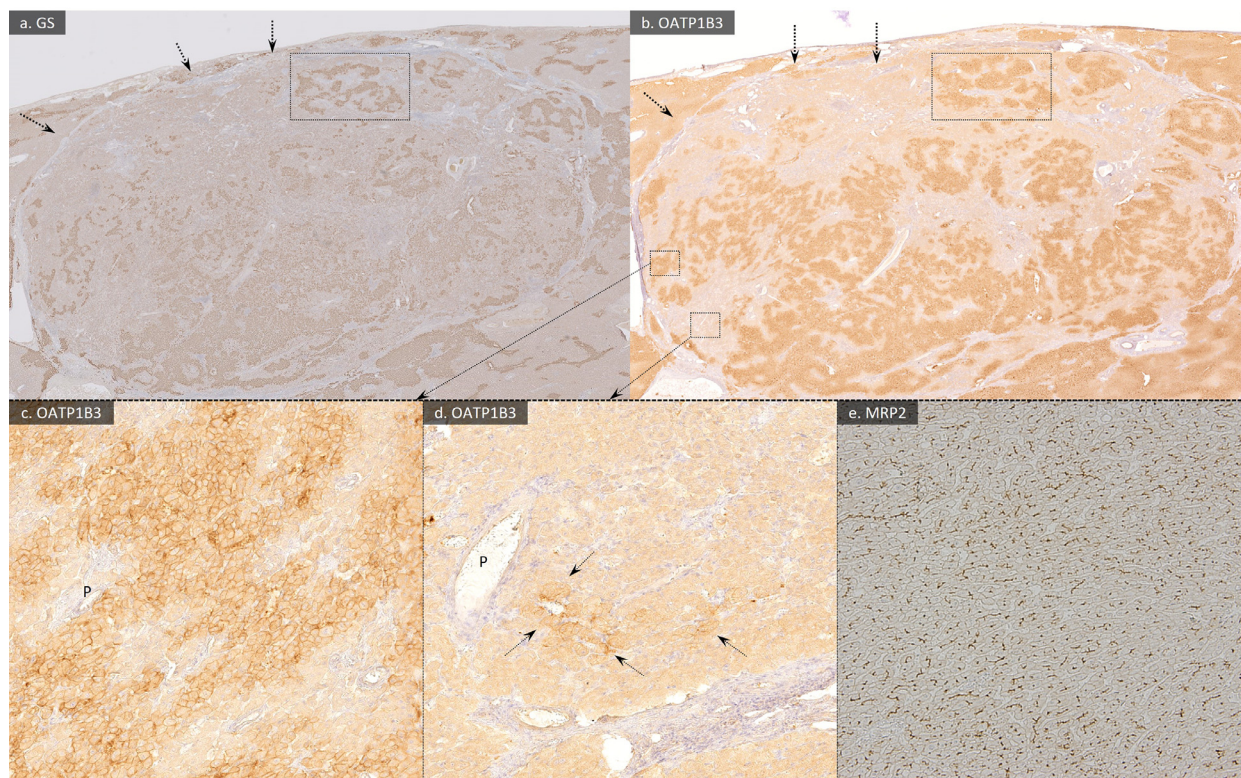
Fig. 5 – Glutamine synthetase (GS) staining, organic anion transporting polypeptide (OATP) 1B3, and multidrug resistance-associated protein (MRP) 2 immunostaining. (A) The GS staining partially shows a map-like staining pattern (original magnification, x 10). (B) OATP1B3 immunostaining seemed to be strongly associated with the findings from the hepatobiliary phase image and showed a similar expression pattern to that of GS (original magnification, x 10). (C, D) The nodule includes a mix of strong (C) and weak (D) membrane expressions (original magnification, x 40). The arrows show the membrane expression of OATP1B3 within a relatively weak expression area (D). (E) The nodule shows a similar expression to the background liver parenchyma on MRP2 staining (original magnification, x 40).

central or hepatic veins surrounding the lesions was not observed. The deformity of the liver, suggesting chronic liver disease, and the central stellate scar and fibrous capsule of the nodule were not identified on any imaging (Figs. 1–3).

Radiologically, hypervascular lesions, such as hepatocellular carcinoma (HCC), hepatocellular adenoma, and FNH, were included in the differential diagnosis; however, the findings were not typical of any hepatic tumor. Because the possibility of malignancy could not be excluded, partial hepatectomy was performed after obtaining informed consent. Histopathological findings were as follows: 1) proliferation of cells similar to normal hepatocytes without nuclear atypia, including proliferation of small bile ducts and unpaired arteries (Fig. 4); 2) normal background liver parenchyma without fibrosis; 3) absence of fibrous capsule and central fibrous scar (Fig. 4); 4) glutamine synthetase (GS) staining showed a map-like staining pattern (Fig. 5); and 5) other immunochemical staining showed similar findings to those of the background liver parenchyma (Fig. 6). These immunochemical findings could rule out hepatocellular adenoma or hepatocellular carcinoma. Immunostaining for organic anion transporter polypeptide (OATP)1B3 showed a similar expression pattern to that of GS (Fig. 5). Multidrug resistance-associated protein 2 (MRP2) immunostaining showed a similar expression to that of background liver

parenchyma (Fig. 5D). Thus, a final diagnosis of FNH-like lesions was established.

Discussion

Here, we describe a case of an FNH-like lesion presenting with unusual inhomogeneous hypointensity accompanied by a scattered isointense area on hepatobiliary phase imaging. Although the terminology has not been fully established, in the present case, the term "FNH-like lesion" was used due to the lack of a central scar, despite other pathological features corresponding to FNH according to the description of the 2019 WHO classification [1].

The general imaging features of FNH correspond well with the histologic features and are similar across modalities. Regarding the histological composition, FNH-like lesions naturally show imaging findings similar to FNH [8]. FNH- and FNH-like lesions revealed a solitary, well-circumscribed, unencapsulated, lobulated mass. Because FNH/FNH-like lesions are mainly composed of hepatocytes, they appear similar to the background liver on unenhanced images; thus, these lesions show iso- to slightly hypo-density on unenhanced CT
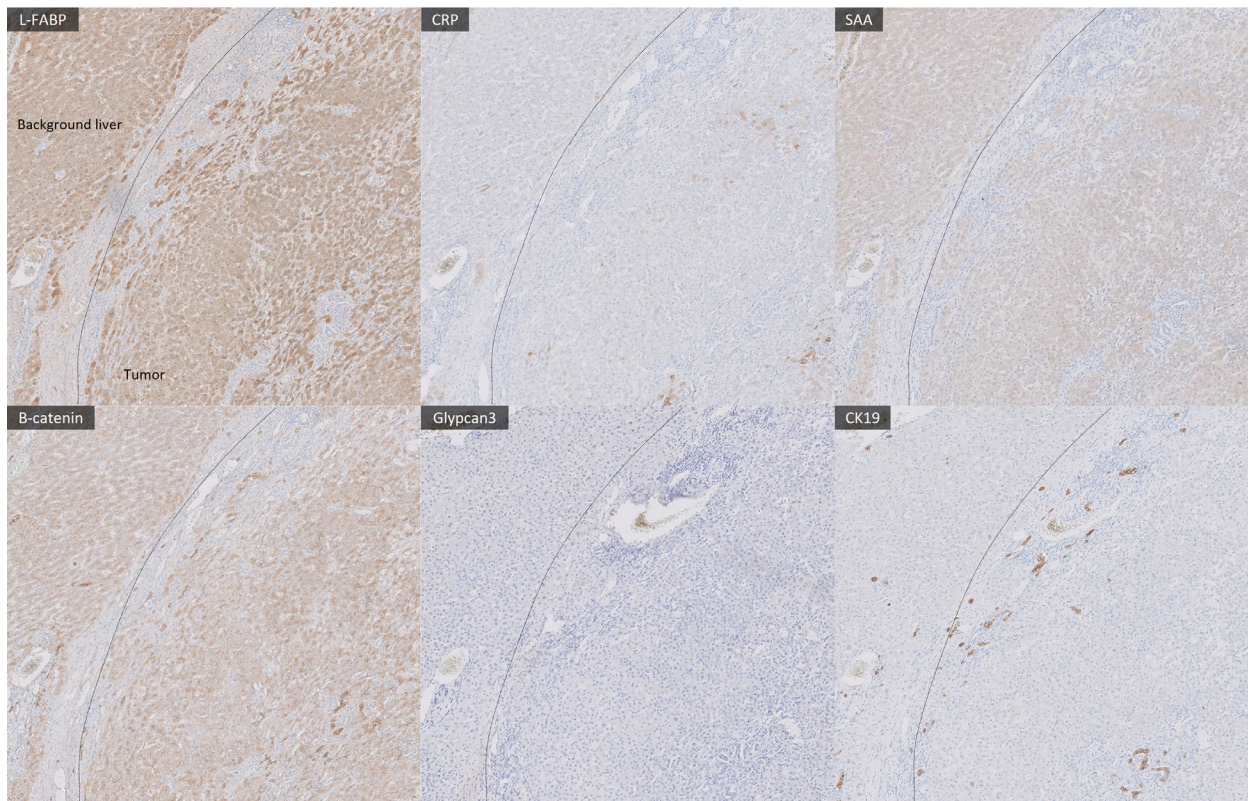
Fig. 6 – Immunohistochemical staining features (original magnification × 20). Tumor cells show the same features as those of the background of the liver using different types of immunohistochemical staining (liver-type fatty acid-binding protein [L-FABP], C-reactive protein [CRP], serum amyloid A [SAA], β-catenin, glypcan 3, and cytokeratin [CK] 19).

images, iso- to slightly hypo-intensity on T1-weighted images, iso- to slightly hyperintense on T2-weighted images [9], or iso- to mildly hyperintense in comparison with the normal liver on diffusion-weighted images [10].

The CT and MRI dynamic contrast studies revealed a characteristic homogeneous arterial phase hyperenhancement. In the portal and delayed/transitional phases, FNH remains slightly hyperenhanced or becomes isoenhanced to the adjacent liver parenchyma [8,9].

Histologically, a central scar composed of fibrous and myxomatous elements is frequently present in FNHs but is visible only in about 60% of lesions on CT and in 80% of the lesions on MRI [8]. In visible cases, the central scar appears as a hyperintense area on T2-weighted images [11]. Imaging findings in the present case were consistent with the above general features of FNH, although a central scar was absent.

Angiography-assisted CT can reveal the characteristic hemodynamics of focal liver lesions [12,13] and can be helpful for differential diagnosis, although angiography-assisted CT has not been widely performed recently because of its invasiveness. In this case, we used this technique to access more details of the hemodynamics of the mass; however, the imaging findings did not narrow the differential diagnosis of hypervascular tumors.

Contrast-enhanced MRI using hepatocyte-specific contrast agents (gadoxetic acid) is generally considered the most sensitive and specific modality for detecting and diagnosing FNH due to the contribution of additional diagnostic information from the hepatobiliary phase [4]. Gadoxetic acid is transported by OATP1B3 (expressed in the sinusoidal membrane of human hepatocytes) [14,15] and exported by MRP2 (expressed on the canalicular side) [16]. The signal intensity of hepatobiliary phase imaging is closely related to the expression of OATP1B3, which transports gadoxetic acid into the sinusoidal membrane of human hepatocytes [15,17]. The influence of MRP2, an export transporter of gadoxetic acid on the canalicular side, is minimal [16]. These can also be applied to FNH and FNH-like lesions [8]. Hyperplastic hepatocytes of FNH and FNH-like lesions maintain the normal functions of hepatocytes, and the characteristics provide the uptake of gadoxetic acid in the lesions, which show iso- or hyperintensity on hepatobiliary phase images [18]. The central scar and a variable number of hepatocytes surrounding it contained no or few functions of uptake of gadoxetic acid and usually showed hypointensity on hepatobiliary phase images [8]. This could be closely related to the zonal variation of the hepatocytes in the hepatic lobes. In normal liver parenchyma, the function of hyperplastic hepatocytes is different between the periportal (zone 1) and the centrilobular areas (zone 3), and OATP1B3 expression is observed predominantly in zone 3 [19]. Although the reason has not been elucidated, hyperplastic hepatocytes surrounding the central scar tend to show the function lo-

cated in zone 1, whereas other hyperplastic hepatocytes of FNH/FNH-like lesions tend to partially present the functions located in zone 3, which shows a map-like distribution. Therefore, FNH has various imaging appearances, depending on the proportions of hyperplastic hepatocytes and central scars, including adjacent hepatocytes. Four major patterns of hepatobiliary phase images have been described for FNH: homogeneous hyperintensity, heterogeneous hyperintensity, homogeneous isointensity, and peripheral ring-like hyperintensity [20,21]. The finding of the hepatobiliary phase in the present case was different from any patterns and made it difficult to diagnose the FNH-like lesions. Moreover, hyperintensity on T2-weighted images was also atypical for FNH-like lesions. Regarding hypervascular hepatic tumors, HCC, the most common hypervascular malignant tumor, is frequently composed of inhomogeneous content due to multinodular configuration, dedifferentiation, degeneration, and necrosis. The heterogeneous nature could present a variety of intensities in the hepatobiliary phase, including hyper-, hypo-, or inhomogeneous intensity [22]. Beta-catenin mutated hepatocellular adenoma, a hypervascular tumor, could show inhomogeneous uptake of gadoxetic acid in the hepatobiliary phase [23]. Therefore, we did not exclude the possibility of HCC or hepatocellular adenoma.

Most previous studies reported that none of the FNHs showed hypointensity relative to the surrounding liver parenchyma in the hepatobiliary phase [24–26], whereas 2.0%-8.8% of FNH did, relative to the surrounding liver parenchyma in other reports [21,27]. The details of FNHs showing hypointensity in the hepatobiliary phase have not been described. Pathological specimens from the present case revealed that the isointense area within the nodule corresponded to the area expressing OATP1B3 on immunostaining, whereas the hypointense area corresponded to the area weakly or not expressing OATP1B3 on immunostaining. These findings corresponded with the previously reported relationship between signal intensity and OATP1B3 expression in FNH/FNH-like lesions [8]. The slightly isointense areas within the hypointense nodule were relatively small but showed a slight uptake of gadoxetic acid compared to the precontrast image. The signal intensity resembled the preserving expression of OATP1B3. Although the mechanism underlying an unknown pattern of hepatobiliary phase image, the hypointense area might be composed of hepatocytes presenting the function of zone 1 in the present FNH-like lesion. Although the mechanism underlying relative hyperintensity on the T2-weighted image was also unclear, the difference between zone 1 and 3 might have been related to the signal intensity.

We should be aware of the unusual findings of FNH and FNH-like lesions on hepatobiliary phase images and carefully examine the hepatobiliary images compared to the precontrast images.

Ethical approval

All procedures followed were in accordance with the ethical standards laid down in the 1964 Declaration of Helsinki and its later amendments.

Patient consent

Informed consent was obtained from the patient for being included in the study.

REFERENCES

[1] Paradis V, Fukayama M, Park YN, Schimacher P. Chapter 8. Tumors of the liver and intrahepatic bile ducts. In: WHO classification of tumors Editorial board; WHO Classification of Tumors, vol. 1 Digestive system tumors. Lyon: IARC Press; 2019. p. 215–64.

[2] Arnason T, Fleming KE, Wanless IR. Peritumoral hyperplasia of the liver: a response to portal vein invasion by hypervascular neoplasms. Histopathology 2013;62:458–64. doi:10.1111/his.12032.

[3] Libbrecht L, Cassiman D, Verslype C, Maleux G, Van Hees D, Pirenne J, et al. Clinicopathological features of focal nodular hyperplasia-like nodules in 130 cirrhotic explant livers. Am J Gastroenterol 2006;101:2341–6. doi:10.1111/j.1572-0241.2006.00783.x.

[4] Suh CH, Kim KW, Kim GY, Shin YM, Kim PN, Park SH. The diagnostic value of Gd-EOB-DTPA-MRI for the diagnosis of focal nodular hyperplasia: a systematic review and meta-analysis. Eur Radiol 2015;25:950–60. doi:10.1007/s00330-014-3499-9.

[5] Reimer P, Schneider G, Schima W. Hepatobiliary contrast agents for contrast-enhanced MRI of the liver: properties, clinical development and applications. Eur Radiol 2004;14:559–78. doi:10.1007/s00330-004-2236-1.

[6] Wanless IR, Mawdsley C, Adams R. On the pathogenesis of focal nodular hyperplasia of the liver. Hepatology 1985;5:1194–200. doi:10.1002/hep.1840050622.

[7] Wanless IR, Albrecht S, Bilbao J, Frei JV, Heathcote EJ, Roberts EA, et al. Multiple focal nodular hyperplasia of the liver associated with vascular malformations of various organs and neoplasia of the brain: a new syndrome. Mod Pathol 1989;2:456–62.

[8] Yoneda N, Matsui O, Kitao A, Kita R, Kozaka K, Koda W, et al. Hepatocyte transporter expression in FNH and FNH-like nodule: correlation with signal intensity on gadoxetic acid enhanced magnetic resonance images. Jpn J Radiol 2012;30:499–508. doi:10.1007/s11604-012-0085-4.

[9] Mortelé KJ, Praet M, Van Vlierberghe H, Kunnen M, Ros PR. CT and MR imaging findings in focal nodular hyperplasia of the liver: radiologic-pathologic correlation. AJR Am J Roentgenol 2000;175:687–92. doi:10.2214/ajr.175.3.1750687.

[10] Dohan A, Soyer P, Guerrache Y, Hoeffel C, Gavini JP, Kaci R, et al. Focal nodular hyperplasia of the liver: diffusion-weighted magnetic resonance imaging characteristics using high b values. J Comput Assist Tomogr 2014;38:96–104. doi:10.1097/RCT.0b013e3182a91006.

[11] Grazioli L, Morana G, Federle MP, Brancatelli G, Testoni M, Kirchin MA, et al. Focal nodular hyperplasia: morphologic and functional information from MR imaging with gadobenate dimeglumine. Radiology 2001;221:731–9. doi:10.1148/radiol.2213010139.

[12] Ueda K, Matsui O, Kawamori Y, Kadoya M, Yoshikawa J, Gabata T, et al. Differentiation of hypervascular hepatic pseudolesions from hepatocellular carcinoma: value of single-level dynamic CT during hepatic arteriography. J Comput Assist Tomogr 1998;22:703–8. doi:10.1097/00004728-199809000-00006.

[13] Miyayama S, Matsui O, Ueda K, Kifune K, Yamashiro M, Yamamoto T, et al. Hemodynamics of small hepatic focal nodular hyperplasia: evaluation with single-level dynamic CT during hepatic arteriography. AJR Am J Roentgenol 2000;174:1567–9. doi:10.2214/ajr.174.6.1741567.

[14] Nassif A, Jia J, Keiser M, Oswald S, Modess C, Nagel S, et al. Visualization of hepatic uptake transporter function in healthy subjects by using gadoxetic acid-enhanced MR imaging. Radiology 2012;264:741–50. doi:10.1148/radiol.12112061.

[15] Leonhardt M, Keiser M, Oswald S, Kühn J, Jia J, Grube M, et al. Hepatic uptake of the magnetic resonance imaging contrast agent Gd-EOB-DTPA: role of human organic anion transporters. Drug Metab Dispos 2010;38:1024–8. doi:10.1124/dmd.110.032862.

[16] König J, Rost D, Cui Y, Keppler D. Characterization of the human multidrug resistance protein isoform MRP3 localized to the basolateral hepatocyte membrane. Hepatology 1999;29:1156–63. doi:10.1002/hep.510290404.

[17] Pascolo L, Petrovic S, Cupelli F, Bruschi CV, Anelli PL, Lorusso V, et al. Abc protein transport of MRI contrast agents in canalicular rat liver plasma vesicles and yeast vacuoles. Biochem Biophys Res Commun 2001;282:60–6. doi:10.1006/bbrc.2001.4318.

[18] Purysko AS, Remer EM, Coppa CP, Obuchowski NA, Schneider E, Veniero JC. Characteristics and distinguishing features of hepatocellular adenoma and focal nodular hyperplasia on gadoxetate disodium-enhanced MRI. AJR Am J Roentgenol 2012;198:115–23. doi:10.2214/AJR.11.6836.

[19] Vander Borght S, Libbrecht L, Blokzijl H, Faber KN, Moshage H, Aerts R, et al. Diagnostic and pathogenetic implications of the expression of hepatic transporters in focal lesions occurring in normal liver. J Pathol 2005;207:471–82. doi:10.1002/path.1852.

[20] van Kessel CS, de Boer E, ten Kate FJ, Brosens LA, Veldhuis WB, van Leeuwen MS. Focal nodular hyperplasia: hepatobiliary enhancement patterns on gadoxetic-acid contrast-enhanced MRI. Abdom Imaging 2013;38:490–501. doi:10.1007/s00261-012-9916-0.

[21] Zech CJ, Grazioli L, Breuer J, Reiser MF, Schoenberg SO. Diagnostic performance and description of morphological features of focal nodular hyperplasia in Gd-EOB-DTPA-enhanced liver magnetic resonance imaging: results of a multicenter trial. Invest Radiol 2008;43:504–11. doi:10.1097/RLI.0b013e3181705cd1.

[22] Vernuccio F, Gagliano DS, Cannella R, Ba-Ssalamah A, Tang A, Brancatelli G. Spectrum of liver lesions hyperintense on hepatobiliary phase: an approach by clinical setting. Insights Imaging 2021;12:8. doi:10.1186/s13244-020-00928-w.

[23] Yoneda N, Matsui O, Kitao A, Kozaka K, Kobayashi S, Sasaki M, et al. Benign hepatocellular nodules: hepatobiliary phase of gadoxetic acid-enhanced MR imaging based on molecular background. RadioGraphics 2016;36:2010–27. doi:10.1148/rg.2016160037.

[24] Mohajer K, Frydrychowicz A, Robbins JB, Loeffler AG, Reed TD, Reeder SB. Characterization of hepatic adenoma and focal nodular hyperplasia with gadoxetic acid. J Magn Reson Imaging 2012;36:686–96. doi:10.1002/jmri.23701.

[25] Grieser C, Steffen IG, Kramme IB, Bläker H, Kilic E, Perez Fernandez CM, et al. Gadoxetic acid enhanced MRI for differentiation of FNH and HCA: a single center experience. Eur Radiol 2014;24:1339–48. doi:10.1007/s00330-014-3144-7.

[26] Kim JW, Lee CH, Kim SB, Park BN, Park YS, Lee J, et al. Washout appearance in Gd-EOB-DTPA-enhanced MR imaging: a differentiating feature between hepatocellular carcinoma with paradoxical uptake on the hepatobiliary phase and focal nodular hyperplasia-like nodules. J Magn Reson Imaging 2017;45:1599–608. doi:10.1002/jmri.25493.

[27] Grazioli L, Bondioni MP, Haradome H, Motosugi U, Tinti R, Frittoli B, et al. Hepatocellular adenoma and focal nodular hyperplasia: value of gadoxetic acid-enhanced MR imaging in differential diagnosis. Radiology 2012;262:520–9. doi:10.1148/radiol.11101742.